The global climate anomaly 1940–1942

Stefan Brönnimann
Institute for Atmospheric and Climate Sciences, ETH, Zürich, Switzerland

In summer 1941, German troops were advancing into the Soviet Union, starting the Eastern Front. In the beginning the troops progressed rapidly, but then an exceptionally harsh winter stopped the assault:

> "1942: The winter comes with full strength, hardly a way left to advance without missing winter equipment. Even the winter clothing is missing. (. . .) At midnight the temperature dropped to a new reported low point. On 24 January 1942, –56 °C was measured at our division observation post." (from the diary of Otto Geipel (Geipel 1997), see also Fig. 1).

The cold European winters during the Second World War (1941/42 was the third in a row) are famous. They even affected the course of the war (Lejenäs 1989). However, it is less well-known that at the same time climate was also anomalous in other regions of the world. Temperatures were exceptionally high in Alaska, and a prolonged El Niño was reported. Moreover, scientists noted unusually high values of total ozone over several European sites. The cold winters in Russia were merely a facet of a global climate anomaly encompassing the troposphere and stratosphere, a fact that was not realised until recently (Brönnimann *et al.* 2004a, Labitzke and van Loon 1999).

Studying past climate variability, especially past climate extremes, is a key to understanding current and future climate change. Apart from the simple (but nevertheless important) aspect of documentation, scientists hope to get insights into the processes underlying such strong climatic events. Analysing the early 1940s anomaly in detail is considered particularly beneficial because of its large spatial scale and its extreme magnitude. Such events have, and will have if they recur in the future, a strong economic and environmental impact. Moreover, this particular event fits well into the current scientific discussion on the role of tropical oceans in the climate system (Alexander *et al.* 2002), on large-scale variability of northern hemispheric climate (Hurrell *et al.* 2003), and on the relation between atmospheric dynamics and stratospheric ozone (Staehelin *et al.* 2001). Studying the 1940–1942 period, therefore, might contribute to a better understanding of the large-scale coupling between tropics and extratropics and between troposphere and stratosphere. Another benefit of such a study is that it involves the development of new tools and techniques for analysing past upper-level climate variability. In this article we summarise our recent work on the 1940–1942 climate anomaly (Brönnimann *et al.* 2004a, b).

How to study upper-level circulation during the early 1940s

One reason why the 1940–1942 period has previously escaped the attention of most climate scientists is that data availability is poor prior to 1948. Almost no earlier upper-air data can be found today in electronic format. However, balloon soundings and other upper-air measurements were made in the 1930s and 1940s, especially during the war (Fig. 2). During their advance towards Moscow, for instance, the German troops performed daily radiosoundings at several sites in the occupied territory. Large

Fig. 1 German soldiers in Russia in January 1942. Temperatures dropped to –56 °C (provided by Barry L. Geipel, www.geipelnet.com/war_albums/otto/).

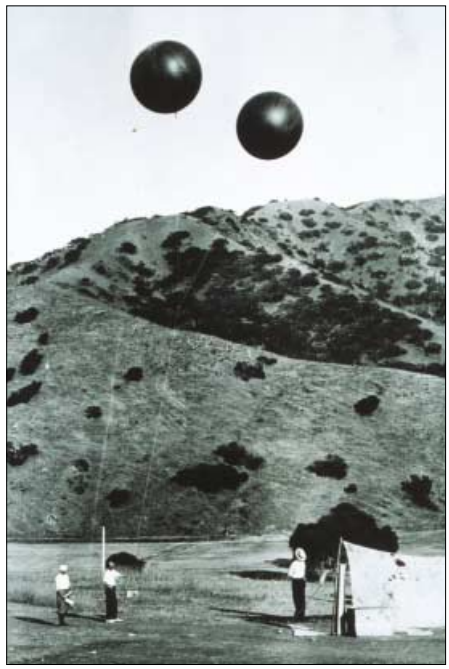

Fig. 2 Early radiosonde launch, USA. Upper-air data from the Second World War and earlier have rarely been analysed and represent a huge potential for climate research (Source: NOAA/Department of Commerce).

aerological networks were in operation in the Soviet Union and the USA. Most of these data can still be found today on paper in various meteorological archives. An example of such a data sheet (from the *German Weather Report*) is shown in Fig. 3. Re-evaluating these data is a very useful, though extremely laborious, job. It includes archive work and literature research in order to locate the data and to obtain as much background information as possible. The data sheets consisting of thousands of pages of often handwritten tables then need to be digitised and checked for errors. The next step is to determine adequate corrections, which are necessary because these early measurements were affected by various instrumental problems. For instance, the large lag of the instruments distorted the profiles and radiosoundings during daytime and suffered from a strong radiation error. Finally, ways must be found to assess and validate the data in order to obtain a product that is adequate for scientific requirements.

These procedures were performed for several tens of thousands of temperature and pressure profiles from aircraft and radiosonde ascents from 1939 to 1944 (Brönnimann 2003). Despite some quality problems (several series were rejected), a relatively good coverage of the northern extratropical troposphere could be achieved (Fig. 4). Unfortunately, many of the balloons did not reach the stratosphere and spatial coverage is much worse above a 10 km altitude. Examples of re-evaluated upper-air data in the form of time-series and profiles are shown in Fig. 5.

It is difficult to address spatial features of the upper-level circulation directly in the radiosonde data; gridded meteorological fields are needed. For this purpose, the historical upper-air data were supplemented with data from the Earth's surface such as temperature measurements or sea-level pressure (SLP) fields. This information (the predictor data) was used in a statistical approach for reconstructing monthly mean upper-level fields (Brönnimann and Luterbacher 2004). The relation between the predictor data and the upper-level fields was derived in a more recent period (NCEP/NCAR re-analysis data 1948–1994, Kistler *et al.* 2001) by means of principal components regression. The obtained transfer functions were then applied to the historical data, yielding monthly mean fields of temperature and geopotential height for the extratropical Northern Hemisphere up to the lower stratosphere (100 mbar). Several upper-air series were not used in the reconstruction approach but were retained for independent validation. Numerous sensitivity studies and validation experiments were performed. It could be shown that the reconstruction skill is generally good, although with seasonal and spatial differences (Brönnimann and Luterbacher 2004).

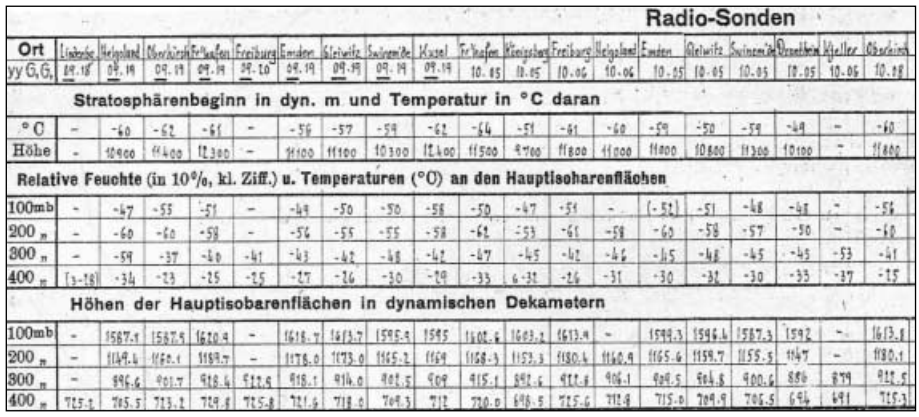

Radio-Sonden

Ort	Lindenberg	Heiligenbeil	Königsberg	Tarnopol	Freiburg	Emden	Gleiwitz	Swinemünde	Kassel	Tarnopol	Königsberg	Freiburg	Heiligenbeil	Emden	Gleiwitz	Swinemünde	Prostken	Kjeller	Oberdürnbach
yy G G	09.18	09.19	09.19	09.19	09.19	09.19	09.19	09.19	09.19	10.05	10.05	10.06	10.06	10.05	10.05	10.05	10.05	10.06	10.05
Stratosphärenbeginn in dyn. m und Temperatur in °C daran																			
°C	-	-60	-62	-61	-	-56	-57	-59	-62	-64	-51	-61	-60	-59	-50	-59	-49	-	-60
Höhe	-	10900	11400	12300	-	11100	11100	10300	12400	11500	9700	11800	11000	11800	10800	11300	10100	-	11800
Relative Feuchte (in 10%, kl. Ziff.) u. Temperaturen (°C) an den Hauptisobarenflächen																			
100mb	-	-47	-55	-51	-	-49	-50	-50	-56	-50	-47	-51	-	(-52)	-51	-48	-48	-	-56
200 „	-	-60	-60	-58	-	-56	-55	-55	-58	-61	-53	-61	-58	-60	-58	-57	-50	-	-60
300 „	-	-59	-37	-60	-41	-43	-42	-48	-42	-47	-45	-42	-46	-45	-48	-45	-45	-53	-41
400 „	[3-18]	-34	-23	-25	-25	-27	-26	-30	-30	-33	4-31	-26	-31	-30	-32	-30	-35	-37	-25
Höhen der Hauptisobarenflächen in dynamischen Dekametern																			
100mb	-	1587.1	1587.9	1620.4	-	1618.7	1613.7	1595.1	1595	1602.6	1603.2	1613.4	-	1598.3	1596.4	1587.3	1592	-	1613.8
200 „	-	1149.6	1160.1	1169.7	-	1178.0	1173.0	1165.2	1169	1158.3	1153.3	1180.4	1160.9	1165.6	1159.7	1155.5	1147	-	1180.1
300 „	-	896.6	901.7	918.4	912.8	918.1	914.0	902.5	909	915.1	897.6	911.8	906.1	908.5	904.8	900.6	886	879	912.5
400 „	715.1	705.5	713.5	729.8	725.8	721.6	718.0	709.3	718	730.0	696.5	715.6	712.8	715.0	709.9	706.5	694	691	715.3

Fig. 3 Excerpt of a data sheet from the German Weather Report*, 10 June 1940, showing radiosonde data from several sites in Europe. For this study, upper-air data from six different sources were digitised.*

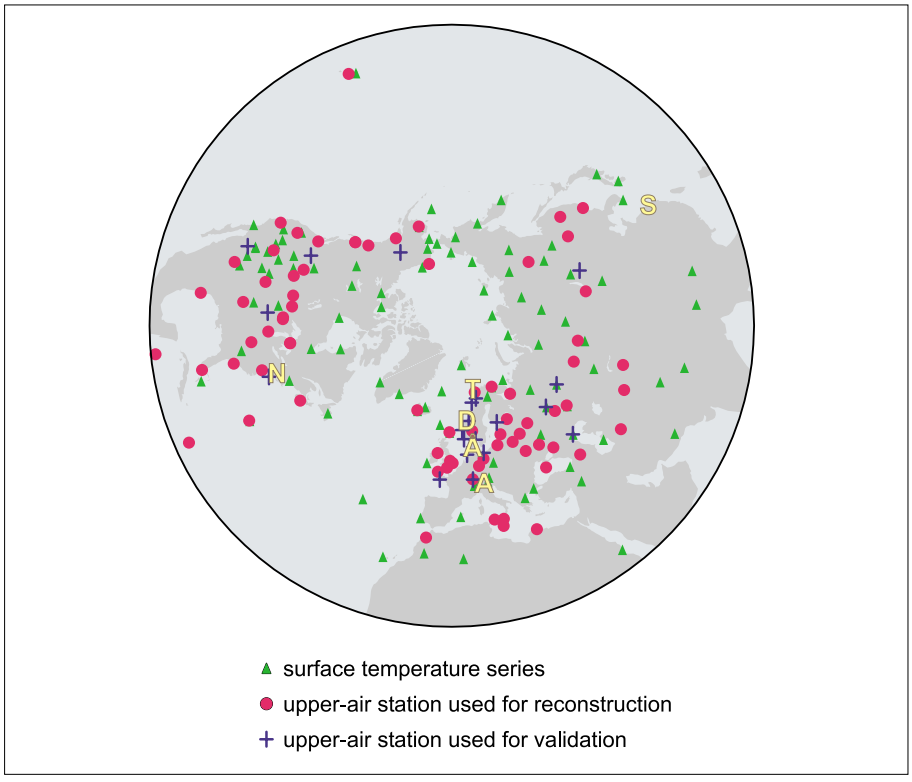

Fig. 4 Upper-air and surface data used for reconstructions and validation. Letters denote total ozone series (A = Arosa, Å = Århus, D = Dombås, N = New York, T = Tromsø, S = Shanghai)

Radiosonde data are not the only source of information on upper-level circulation. Indirect information can also be derived from total ozone, a quantity that has been measured for almost 80 years (Fig. 6). In the absence of strong ozone-depleting chemistry, total ozone at northern mid-latitudes is controlled by stratospheric transport processes (Staehelin *et al.* 2001), which in some cases can be diagnosed in the data. For our study we used six historical total ozone series from the 1930s and 1940s that were recently re-evaluated in the context of this and other projects (Staehelin *et al.* 1998, Svendby 2003, Brönnimann *et al.* 2003).

Results: a global climate anomaly

The climate of the 1940–1942 period has until now, only been studied from regional viewpoints, addressing the anomalies in the Pacific region (Bigg and Inoué 1992) or in Europe (Lejenäs 1989). The new data now show for the first time that the anomaly of the early 1940s encompassed the troposphere and stratosphere of the entire world (Brönnimann *et al.* 2004a). One remarkable feature was the persistence of the anomaly features, especially at the Earth's surface, through all seasons over a period of more than two years, i.e. from around January 1940 to February 1942 (Supplementary Fig.1 in Brönnimann *et al.* 2004a). Fig. 7(b) shows anomalies (with respect to the 1961–1990

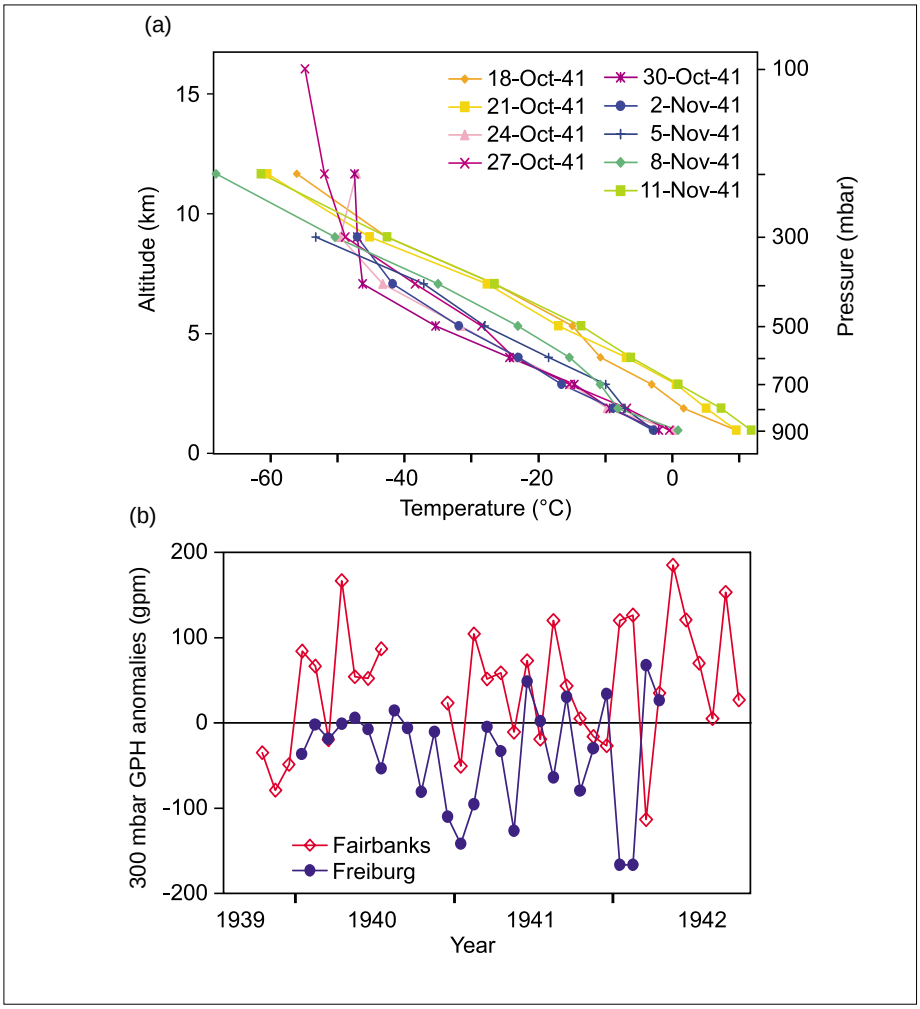

Fig. 5 Historical radiosonde data. (a) Sequence of profiles (one profile every three days is displayed) during a cold spell in autumn 1941 at Freiburg, Germany. (b) Monthly series of 300 mbar geopotential height at Freiburg, Germany, and Fairbanks, Alaska (anomalies with respect to 1961–1990).

Fig. 6 Total ozone measurements at Arosa, Switzerland, during an intercomparison around 1952. Historical total ozone data such as the series from Arosa, which goes as far back as 1926, provide important information on the past variability of the stratosphere (Source: LKO Arosa, MeteoSwiss).

mean annual cycle) of surface temperature and SLP averaged for this period. In Europe, extreme negative anomalies appear in the averaged temperature field mainly due to cold winters, including the two coldest of the twentieth century in many regions. Low temperatures were also registered in other seasons. An example of a strong and prolonged cold spell in autumn 1941 is shown in Fig. 5(a) in the temperature profiles from Freiburg (Germany). Climate was also anomalous elsewhere in the northern extratropics. Very high temperatures were observed in Alaska (Fig. 8) and Canada, including the warmest winter of the twentieth century in parts of Alaska, as well as in Central Asia. Low temperatures were registered in the central North Pacific, where 1940 and 1941 were the coldest two years of the twentieth century, and in northern Siberia. Anomalous climate was not only observed in the northern extratropics, but also in the tropical Pacific region. A strong and prolonged El Niño lasted from autumn 1939 to spring 1942 (Fig. 7). Climate was also anomalous in the Southern Hemisphere (not shown), with low sea surface temperatures at mid-latitudes in all ocean basins being the most pronounced feature.

The temperature deviations at the Earth's surface are in excellent agreement with the anomalies in the SLP field. The main features are a strong Aleutian low, a weak Icelandic low, and high pressure over Scandinavia. The intensified Aleutian low led to anomalous warm air advection in its front, contributing to increased temperatures in Alaska. The weak Icelandic low and high SLP over Scandinavia are in agreement with more frequent blocking and cut-off lows and advection of continental cold air to Eastern Europe (Lejenäs 1989). This configuration of pressure anomalies over the Pacific-North American sector is well-known as the positive mode of the so-called Pacific-North American pattern, whereas the anomalies over the Atlantic-European sector are related to the negative phase of the North Atlantic Oscillation (NAO) (Hurrell *et al.* 2003). The two circulation patterns are normally considered independent and hence concurrent strong anomalies in the Pacific region and Europe are noteworthy.

Reconstructed upper-tropospheric fields (not shown) provide evidence of a change in the planetary wave structure (Brönnimann *et al.* 2004a). Higher up, at 100 mbar (around 16 km altitude) in the extratropical lower stratosphere, the circulation is normally dominated by the wintertime polar vortex. The reconstructed geopotential height fields for this level (Fig. 7(a)) show that the vortex was weak and meridionally expanded in all three winters, as well as in the mean over the period (positive pressure anomalies over the polar region, negative at mid-

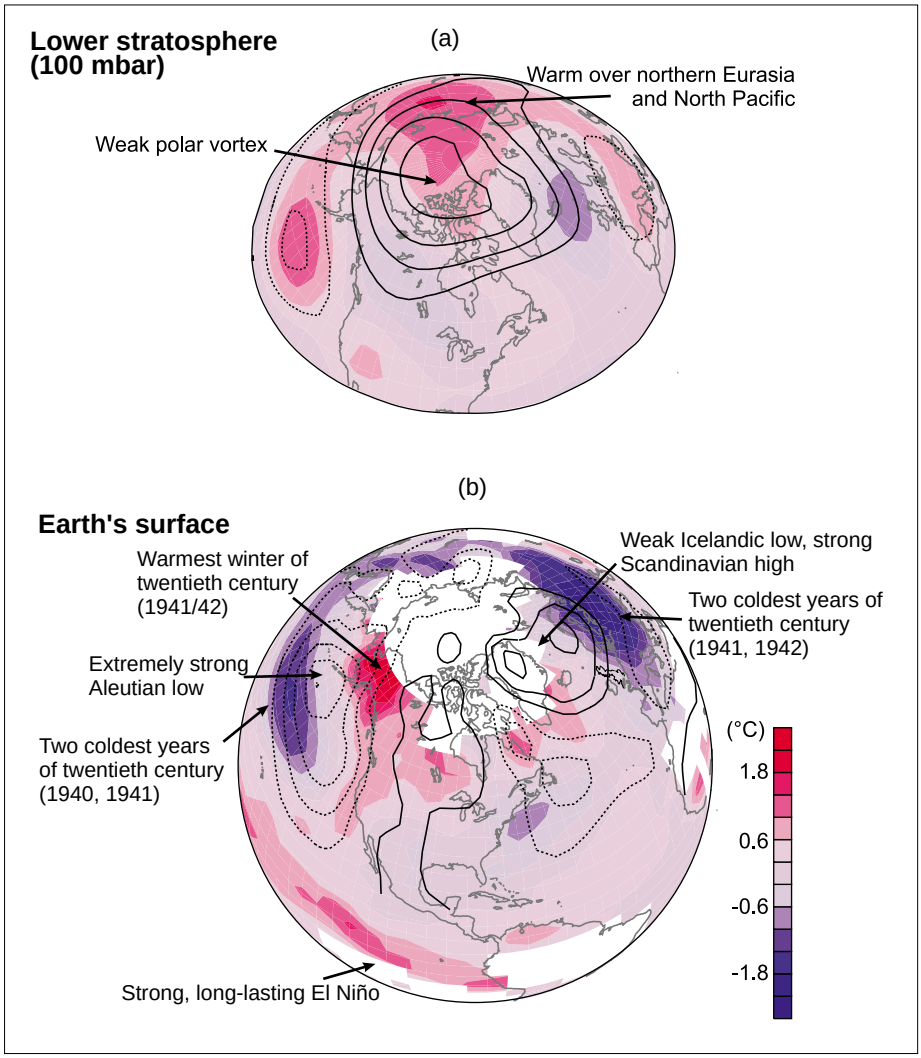

Fig. 7 Averaged anomaly fields (with respect to 1961–1990) from January 1940 to February 1942 of (a) temperature and geopotential height (contours, interval 20 gpm, zero contour not shown) at 100 mbar and (b) surface temperature (HadCRUT2v, Jones and Moberg 2003) and SLP (contours, interval 1 mbar, zero contour not shown, Trenberth and Paolino 1980).

Fig. 8 Parade on 4 July 1940 in Anchorage, Alaska. With an average temperature of 3.4 °C, 1940 was one of the warmest years of the twentieth century in Anchorage. (Photo courtesy of Russ Dow, provided by the 3rd Wing, Elmendorf Air Force Base, Alaska.)

latitudes). This is in agreement with a weak Icelandic low at the Earth's surface (or the negative phase of the NAO). The 100 mbar temperature field also showed a characteristic pattern in 1940–1942, with positive anomalies over northern Eurasia and the northern North Pacific and negative anomalies over parts of the North Atlantic and Canada (Brönnimann *et al.* 2004a). At mid-latitudes, this pattern partly reflects the planetary wave structure. Lower stratospheric temperatures tend to be higher above upper-tropospheric troughs, when the tropopause descends to low altitudes (they are often anticorrelated with tropospheric temperatures, see for instance Fig. 5(a)). In the polar region in winter other processes dominate. The warming in northern Siberia was probably related to the weak polar vortex.

Although no meteorological data are available above 100 mbar, there are indications of an anomalous circulation in the middle stratosphere (30–10 mbar or 25–33 km). Evidence suggests major midwinter stratospheric warmings in each of the three winters, i.e. at least in January 1940, February 1941 and February 1942 (Brönnimann *et al.* 2004b). This is comparably frequent, as such events occurred only every third winter on average in the past 50 years. Major midwinter warmings are defined as a complete collapse of the polar vortex in the middle stratosphere, often accompanied by sudden warmings of 30–40 °C within a few days (Labitzke and van Loon 1999). Though rare, these events are important as they may propagate downward and affect tropospheric circulation (Polvani and Waugh 2004). Another indication for a stratospheric anomaly arises from historical total ozone data (Fig. 9). All six available series show a peak in 1940–1942, at sites as far apart as China, North America, central Europe, and the Arctic (Brönnimann *et al.* 2004a). This cannot be explained by chemical processes, but points to anomalous ozone transport and hence an anomalous stratospheric circulation.

In summary, the cold winters in Europe in 1940–1942 were not the only climatic anomaly in this period. Surface and upper-air data show strong deviations of temperature and pressure all over the northern extratropics as well as in the tropics. Moreover, the historical upper-air data provide evidence that the anomaly extended up to the stratosphere. The 1940–1942 period can therefore be addressed as an extreme anomaly of the global troposphere-stratosphere system. Accordingly, the event had far reaching economic and environmental impacts. Apart from affecting the Second World War (see above), the climatic anomalies caused major flooding in Peru, severe drought in the Sahel region, some of the most extensive wildfires on record in

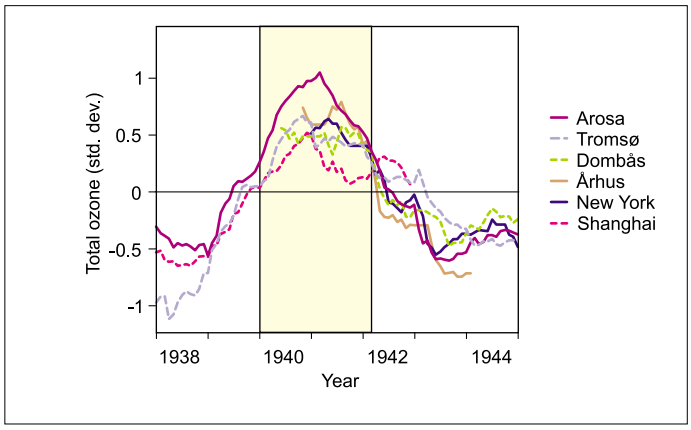

Fig. 9 Standardised monthly total ozone anomalies (with respect to all available data in the 1938–1944 period), smoothed with a 2-year moving average (12 values must be non-missing). The period January 1940 to February 1942 is marked. See Brönnimann et al. *(2004a,b) for data references.*

Alaska (Kasischke *et al.* 1993), as well as drought and crop failure in Borneo and Australia. Catches of several commercial fish species (Pacific salmon, sardine) continued to be exceptionally high during these years, owing in part to the anomalous ocean temperatures in the North Pacific (Klyashtorin 2001).

In order to analyse the 1940–1942 anomaly in the context of twentieth century climate variability, several indices were formed that capture the main features of the 1940–1942 anomaly and allow the drawing of time-series for the twentieth century (Fig. 10). In order to focus on the timescale of this unusual event and to account for its persistence, all series were smoothed with a 2-year moving average (see Brönnimann *et al.* (2004a) for an analysis based on seasonal and annual averages). These series include the widely used El Niño index NINO3.4 (sea surface temperatures averaged over the region 120–170° W/5° S–5° N from Kaplan *et al.* 1998), surface air temperature averaged over central, northern and eastern Europe termed T_{Euro} (10–55° E/45–70° N, Jones and Moberg 2003), the wintertime difference between the SLP anomalies of the Icelandic and Aleutian lows (IL-AL), a measure for the 'weakness' of the polar vortex at 100 mbar (Z100) in winter, and total ozone at Arosa (see figure caption for further details). The anomalies in the early 1940s were clearly extreme on the chosen time-scale. This holds especially for T_{Euro} and for the seesaw between Icelandic and Aleutian low. In both series, the 1940–1942 peak was far outside the variability encountered otherwise in the twentieth century. The same is true for total ozone at Arosa, the longest available series. The years 1940 and 1941 had the highest annual mean values on record. NINO3.4 also exhibits an absolute maximum in the early 1940s, which is due to both the strength and the long duration of this El Niño event (in fact, the 1982/83 and 1997/98 El Niños were stronger, but shorter).

Was it a coincidence – or El Niño?

What caused the 1940–1942 climate anomaly? Was it just the coincidence of a strong El Niño affecting the Pacific region and concurrent, but unrelated, climate variations in the Atlantic-European sector? Or were the anomalies in Europe and the stratosphere related to El Niño? The features in the Pacific-North American sector can, to a large extent, be explained by El Niño through changes in the Hadley circulation and Rossby wave generation. These relationships are relatively well-documented (e.g. Alexander *et al.* 2002). Possible El Niño effects on Europe are less certain. According to several observational and modelling studies, the expected El Niño winter signal in Europe consists of cold temperatures in Northern Europe, high SLP from Iceland to Scandinavia and low SLP over central and Western Europe (Fraedrich and Müller 1992, Merkel and Latif 2002). Also, strong El Niños have been found to be associated with a weak polar vortex and more frequent major stratospheric warmings (van Loon and Labitzke 1987). Hence, all anomalies found in the 1940–1942 period, both at the surface and in the stratosphere, are in agreement with a possible El Niño effect. However, other studies find no consistent signal and results are controversial, or even contradictory, at times. Detecting an El Niño signal in Europe, far from the El Niño region, is difficult because the variability of the northern extratropical circulation is very large and at the same time the number of strong El Niño events is small. Moreover, strong volcanic eruptions as well as the anthropogenic greenhouse effect and stratospheric ozone depletion might interfere with an El Niño effect, especially in recent decades. It has also been suggested that the signal itself is non-stationary, i.e. that the effect of El Niño on European climate is not the same at different times (Graetbach *et al.* 2004). Almost certainly, it depends on the state and history of the circulation over the Atlantic-European sector at the time of the onset of El Niño.

To some extent, this uncertainty in the global extent of El Niño effects is also reflected in our selected index series. Analysing the data for the past 50 years it becomes clear that not all El Niños show the same features as the one in 1940–42. There is a tendency for El Niño events to be associated with below-normal temperatures in north-eastern Europe, a weak Icelandic low and strong Aleutian low, a weak polar vortex (high Z100) and above-normal total ozone at Arosa. For instance, the El Niños of 1969/70, 1976/78, 1986/87, and to some extent 1997/98 show this behaviour. An opposite tendency is observed for La Niña events. However, other strong El Niño events (e.g. 1982/83) show a different pattern.

Climate models offer an alternative way of studying possible relations between El Niño, North Pacific and European climate, and the northern stratosphere. We analysed the 650-year control run of the coupled climate model (CCSM-2.0) (see Brönnimann *et al.*, 2004a). The model consists of ocean, atmosphere, land surface, and sea-ice modules and produces a realistic 'natural' climate variability, including a good representation of El Niño. From the model output, the same index series as shown for the observations were calculated, smoothed with a 2-year moving average, and analysed with respect to their extremes. As to El Niño (NINO3.4), the three highest peaks are comparable to the 1940s, not only with respect to the strength (smoothed series >1.2 deg C), but also the duration (25–37 consecutive months >0 °C) and maximum values (2.4–2.6 deg C, which is slightly stronger than in 1940–1942). Each exhibits all the major features of the 1940–1942 period in comparable strength, which is very remarkable. To obtain a larger sample of 'strong El Niños', the threshold was lowered. The 11 NINO3.4 peaks above 0.9 deg C (comparable to the 1997/98 or 1986/87 events) exhibit highly significant deviations with respect to all analysed series (the same result is found when addressing the year-to-year timescale, focusing on winter only; see Brönnimann *et al.* (2004a)). This is shown in Fig. 10 (right), where composite series, centred on the peak in the smoothed NINO3.4 index, and their respective 95% confidence intervals are displayed. Each of the 11 strong El Niños was accompanied by exceptionally low T_{Euro}. The Icelandic low and stratospheric polar vortex were weakened in ten and nine cases, respectively.

The same characteristic anomalies as in the 1940s thus appear consistently in the model.

Averaged anomaly fields at the surface and the 100 mbar level for the selected strong El Niños in the model (11 2-year periods, thus corresponding to year 0 in Fig. 10, right) are shown in Fig. 11. A comparison of this figure with Fig. 7 reveals strong similarities. To sum up, most of the features of the climate anomaly 1940–1942, at the surface as well as in the stratosphere, are produced by a coupled climate model during strong and prolonged El Niño events. This shows that the concurrence of climate extremes in the tropical and North Pacific, Europe, and the northern stratosphere in the early 1940s was not a coincidence. Rather, it represents a consistent extreme state of the global troposphere-stratosphere system on inter-annual time-scales related to strong El Niños. It is not the only possible mode of the global circulation in a state of strong, prolonged El Niño, as the observations from the past 50 years show, but it is a consistent and recurring mode.

The role of planetary waves

Of particular interest is the coupling between troposphere and stratosphere and the relation between El Niño and total ozone. Unfortunately, the CCSM-2.0 model does not simulate total ozone, but it facilitates the study of dynamical properties related to wintertime troposphere-stratosphere coupling. It could be shown that increased early-to-midwinter meridional eddy heat flux at 100 mbar accompanies the strongest model El Niños (Brönnimann *et al.*, 2004a). This is a measure for upward propagating planetary wave activity reaching the stratosphere and interacting with the mean flow. More wave activity is expected to slow down the zonal (westerly) circulation and enhance the meridional (poleward) circulation in the middle stratosphere and downwelling over the polar region. This affects lower stratospheric temperature and pressure fields and results in a weak polar vortex and high Arctic temperatures in spring (Newman *et al.* 2001). Moreover, pulses of increased wave activity flux are the trigger for most major stratospheric warmings (Polvani and Waugh 2004) and hence more frequent warmings are expected. All of this is consistent with observations from the early 1940s. Results must remain tentative, however, as the 1940s data do not allow the direct calculation of eddy heat fluxes.

A strengthened meridional circulation and increased downwelling over the polar region also affect total ozone (Randel *et al.* 2002). More ozone is transported in the middle stratosphere from the tropical source regions to the extratropics (a stronger Brewer–Dobson circulation) and the ozone column over the Arctic is increased due to downwelling. As a consequence, high total ozone is expected especially over the Arctic, but also at mid-latitudes, consistent with

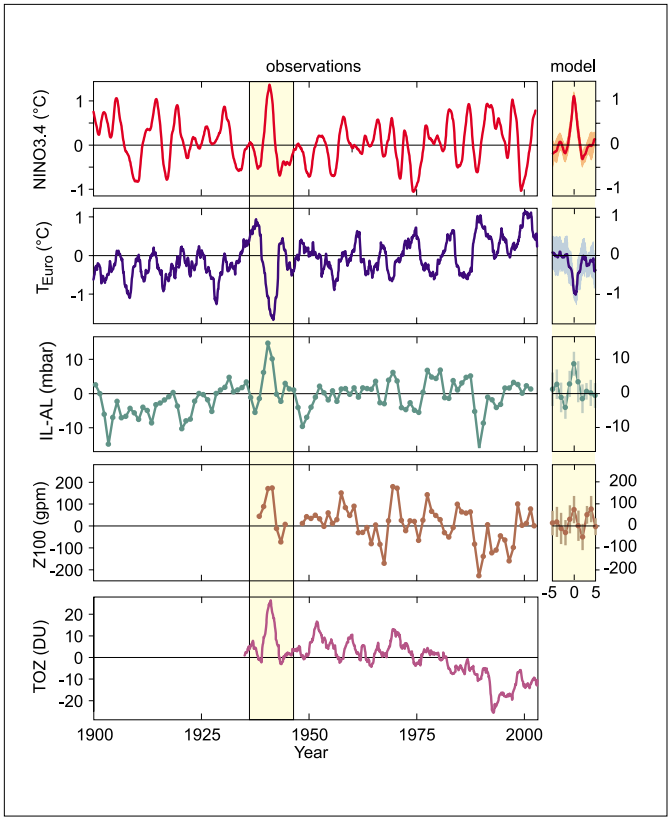

Fig. 10 Index time-series characterising the 1940–1942 anomaly. Left: Observations, right: strong model El Niños (mean and 95% confidence interval for the 11 strongest peaks in the smoothed NINO3.4 series). NINO3.4 is an El Niño index (sea surface temperatures averaged over the region 120–170° W/5°S–5°N), T_{Euro} is surface air temperature averaged over central, northern and eastern Europe (10–55° E/45–70° N), IL-AL is the Jan.–Apr. average of the SLP (Trenberth and Paolino 1980) difference between Iceland (10°–40°W/60°–70°N) and the Aleutians (140°–170°W/40°–55°N). Z100 is the Jan.–Apr. average of the 100 mbar geopotential height difference between 75°–90°N and 40°–55°N (Brönnimann and Luterbacher 2004), TOZ is total ozone at Arosa (Staehelin et al. *1998). All series are anomalies with respect to 1961–1990, smoothed with a 2-year (2-point for IL-AL, Z100) moving average (see Brönnimann* et al. *2004a).*

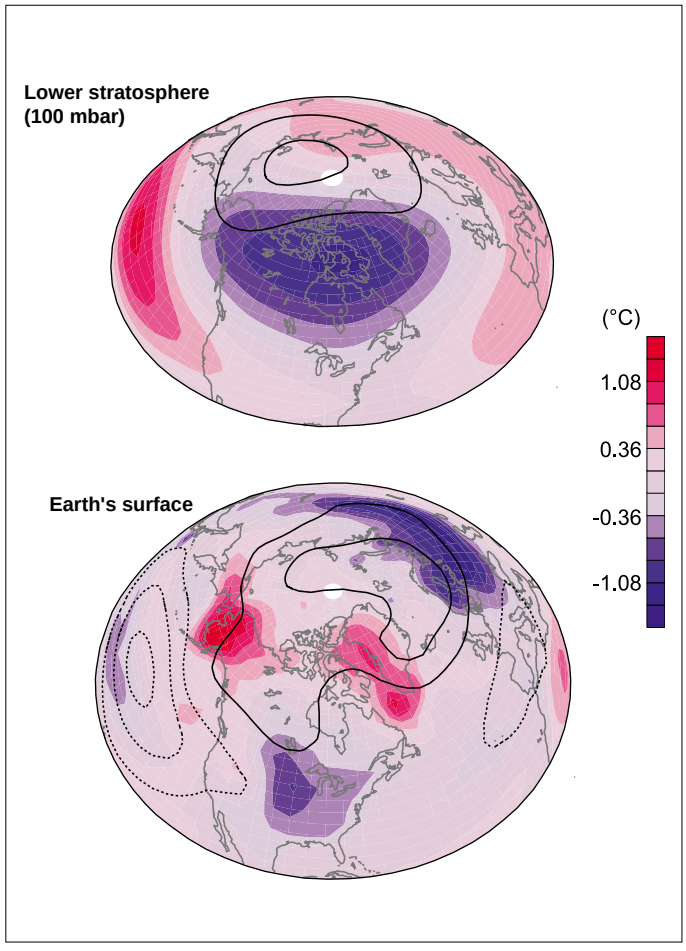

Fig. 11 Same as Fig. 7 for the 11 strongest model El Niños (11 2-year periods centred on the peak in the smoothed NINO3.4 series).

observations from the early 1940s. However, it should be noted that another effect also contributed to high total ozone at mid-latitudes, namely ozone redistribution in the lower stratosphere related to changes in planetary wave structure. Frequent upper-trough situations over central Europe (during which the stratospheric column is increased) were probably the main cause for the total ozone peak at Arosa (Fig. 10). Planetary waves play a crucial role in ozone-climate relations both through regional scale ozone redistribution in the lower stratosphere and planetary scale transport in the middle stratosphere. The early 1940s provide illuminative examples for both processes.

Conclusions

The study of an extreme climatic anomaly in the early 1940s demonstrates that strong and prolonged El Niño events can affect the global troposphere and stratosphere in a very characteristic way, with far-reaching environmental and economic impacts. Although data from the past 50 years show that not all El Niño events lead to such extreme periods, the agreement between the 1940–1942 period and strong El Niño events in a coupled climate model simulation is striking. The global climate anomaly in 1940–1942 was unprecedented in strength, yet exemplary in character, providing a unique opportunity to study large-scale climate variability.

Acknowledgements

The research was funded by the Swiss National Science Foundation and the Holderbank and Janggen-Poehn Foundations. The author thanks J. Luterbacher, J. Staehelin, T. M. Svendby, G. Hansen and T. Svenøe for fruitful collaboration. The CCSM-2.0 control run b20.007 was provided by the University Corporation for Atmospheric Research, Boulder, Colorado.

References

Alexander, M. A., Blade, I., Newman, M., Lanzante, J. R., Lau, N.-C. and Scott, J. D. (2002) The atmospheric bridge: Influence of ENSO teleconnnections on air-sea interaction over the global oceans. *J. Clim.*, **15,** pp. 2205–2231

Bigg, G. R. and Inoué, M. (1992) Rossby waves and El Niño during 1935–46. *Q. J. R. Meteorol. Soc.,* **118,** pp. 125–152

Brönnimann, S. (2003) A historical upper-air data set for the 1939–1944 period. *Int. J. Climatol.,* **23,** pp. 769–791

Brönnimann, S. and Luterbacher, J. (2004) Reconstructing Northern Hemisphere upper-level fields during World War II. *Clim. Dyn.*, **22,** pp. 499–510

Brönnimann, S., Cain, J. C., Staehelin, J. and Farmer, S. F. G. (2003) Total ozone observations prior to the IGY. II: Data and quality. *Q. J. R. Meteorol. Soc.*, **129,** pp. 2819–2843

Brönnimann, S., Luterbacher, J., Staehelin, J., Svendby, T. M., Hansen, G. and Svenøe, T. (2004a) Extreme climate of the global troposphere and stratosphere in 1940–42 related to El Niño. *Nature*, **431,** pp. 971–974

Brönnimann, S., Luterbacher, J., Staehelin, J. and Svendby, T. M. (2004b) An extreme anomaly in stratospheric ozone over Europe in 1940–1942. *Geophys. Res. Lett.,* **31,** L08101, doi: 10.1029/2004GL019611

Fraedrich, K. and Müller, K. (1992) Climate anomalies in Europe associated with ENSO extremes. *Int. J. Climatol.*, **12,** pp. 25–31

Geipel, B. L. (1997) The Russian Campaign 1941–1945, A photo diary by Otto, 3rd Company, 7th PanzerJaeger Battalion (Later 1007 Sturmgeschutz Abteilung), 7th Bavarian Infantry Division (Munich) (http://www.geipelnet.com/war_albums/otto/ow_12.html, accessed Dec. 2003)

Graetbatch, R. J., Lu, J. and Peterson, K. A. (2004) Nonstationary impact of ENSO on Euro-Atlantic winter climate. *Geophys. Res. Lett.,* **31,** L02208, doi:10.1029/2003GL018542

Hurrell, J., Kushnir, Y., Ottersen, G. and Visbeck, M. (eds.) (2003) *The North Atlantic Oscillation. Climatic Significance and Environmental Impact.* AGU, Washington DC

Jones, P. D. and Moberg, A. (2003) Hemispheric and large-scale surface air temperature variations: An extensive revision and an update to 2001. *J. Clim.*, **16,** pp. 206–223

Kaplan, A., Cane, M., Kushnir, Y., Clement, A., Blumenthal, M. and Rajagopalan, B. (1998) Analyses of global sea surface temperature 1856–1991. *J. Geophys. Res.*, **103,** pp. 18567–18589

Kasischke, E. S., French, N. H. F., Harrell, P., Christensen, N. L., Ustin, S. L. and Barry, D. (1993). Monitoring of wildfires in Boreal Forests using large area AVHRR NDVI composite image data. *Remote Sens. Environ.*, **45,** pp. 61–71

Kistler, R. and 12 co-authors. (2001) The NCEP-NCAR 50-year reanalysis: Monthly means CD-ROM and documentation. *Bull. Am. Meteorol. Soc.*, **82,** pp. 247–268

Klyashtorin, L. B. (2001) *Climate change and long-term fluctuations of commercial catches - the possibility of forecasting*. FAO Fisheries Technical Paper 410, Rome

Labitzke, K. G. and van Loon, H. (1999) *The stratosphere. Phenomena, History, and Relevance*. Springer, Berlin

Lejenäs, H. (1989) The severe winter in Europe 1941–1942: The large-scale circulation, cut-off lows, and blocking. *Bull. Am. Meteorol. Soc.,* **70,** pp. 271–281

Merkel, U. and Latif, M. (2002) A high resolution AGCM study of the El Niño impact on the North Atlantic/European sector. *Geophys. Res. Lett.*, **29,** 1291, doi:10.1029/2001GL013726

Newman, P. A., Nash, E. R. and Rosenfield, J. (2001) What controls the temperature of the arctic stratosphere during the spring? *J. Geophys. Res.*, **106,** pp. 19999–20010

Polvani, L. M. and Waugh, D. W. (2004) Upward wave activity flux as precursor to extreme stratospheric events and subsequent anomalous surface weather regimes. *J Clim.*, **17,** pp. 3548–3554

Randel, W. J., Wu, F. and Stolarski, R. (2002) Changes in column ozone correlated with the stratospheric EP flux. *J. Meteorol. Soc. Jpn.,* **80,** pp. 849–862

Staehelin, J., Renaud, A., Bader, J., McPeters, R., Viatte, P., Hoegger, B., Bugnion, V., Giroud, M. and Schill, H. (1998) Total ozone series of Arosa (Switzerland). Homogenization and data comparison. *J. Geophys. Res.,* **103,** pp. 5827–5841

Staehelin, J., Harris, N. R. P., Appenzeller, C. and Eberhard, J. (2001) Ozone trends: A review. *Rev. Geophys.*, **39,** pp. 231–290

Svendby, T. M. (2003) Reanalysis of total ozone measurements at Dombås and Oslo, Norway, from 1940 to 1949. *J. Geophys. Res.*, **108,** 4750, doi:10.1029/2003JD003963

Trenberth, K. E. and Paolino, D. A. (1980) The Northern Hemisphere sea level pressure data set: Trends, errors, and discontinuities. *Mon. Wea. Rev.*, **108,** pp. 855–872

van Loon, H. and Labitzke, K. (1987) The Southern Oscillation. Part V: The anomalies in the lower stratosphere of the Northern Hemisphere in winter and a comparison with the Quasi-Biennial Oscillation. *Mon. Wea. Rev.*, **115,** pp. 357–369

Correspondence to: Stefan Brönnimann, Institute for Atmosphere and Climate Sciences, ETH, Zürich, Switzerland

e-mail: stefan.brönnimann@env.ethz.ch

doi: 10.1256/wea.248.04